Heliyon 10 (2024) e37168

Contents lists available at ScienceDirect

Heliyon

journal homepage: www.cell.com/heliyon

Research article

Multi-omic analyses identified SFRP4 as a novel biomarker in abnormal uterine bleeding with ovulatory dysfunction

Yunxiu Zhao [a,c,1], Yifei Lv [a,c,1], Yizhou Huang [b,c], Tao Zhang [b,c], Yibing Lan [b,c], Chunming Li [b,c], Peiqiong Chen [b,c], Wenxian Xu [b,c], Linjuan Ma [b,c,2,**], Jianhong Zhou [b,c,*,2]

[a] *Department of Gynecology, Women's Hospital, Zhejiang University School of Medicine, Key Laboratory of Women's Reproductive Health of Zhejiang Province, Hangzhou, China*
[b] *Department of Gynecology, Women's Hospital, Zhejiang University School of Medicine, Hangzhou, China*
[c] *Zhejiang Provincial Clinical Research Center for Obstetrics and Gynecology, China*

ARTICLE INFO

Keywords:
Multi-omic analyses
Abnormal uterine bleeding with ovulatory dysfunction (AUB-O)
Abnormal uterine bleeding with atypical hyperplasia/malignancy (AUB-M)
Secreted frizzled-related protein 4 (SFRP4)
Wnt pathway

ABSTRACT

The goal of the study was to explore the mechanism underlying the progression from abnormal uterine bleeding with ovulatory dysfunction (AUB-O) to AUB with atypical hyperplasia/malignancy (AUB-M). AUB-O, AUB-M and control endometrial tissues were subjected to multi-omic analyses to identify biomarkers. Differentially expressed genes (DEGs) and differentially expressed proteins (DEPs), including SFRP4, between the AUB-O and AUB-M groups were identified. The expression of SFRP4 was upregulated in endometrial tissues from AUB-O groups compared to that from AUB-M groups. SFRP4 knockdown in human endometrial epithelial cells (hEECs) promoted cell migration, invasion, proliferation and colony formation but inhibited apoptosis. Furthermore, the levels of key Wnt pathway proteins were altered by SFRP4 knockdown: Wnt-5A was downregulated and Wnt-7A was upregulated. In conclusion, we identified SFRP4 as an AUB-O-related molecule. SFRP4 might play a key role in hEECs apoptosis, migration, invasion, proliferation and colony formation via the Wnt pathway. SFRP4 may serve as a repressive factor regarding the progression of AUB-O to AUB-M. However, further studies are warranted to elucidate the exact mechanism.

Abbreviations: AUB-O, abnormal uterine bleeding with ovulatory dysfunction; AUB-M, abnormal uterine bleeding with atypical hyperplasia/malignancy; qRT-PCR, quantitative reverse transcription polymerase chain reaction; DEGs, differentially expressed genes; DEPs, differentially expressed proteins; EC, endometrial cancer; PBS, phosphate-buffered saline; ACN, acetonitrile; TFA, trifluoroacetic acid; DAB, diaminobenzidine; GO, Gene Ontology; KEGG, Kyoto Encyclopedia of Genes and Genomes; SFRP4, secreted frizzled-related protein 4; AEH, atypical endometrial hyperplasia; ANOVA, analysis of variance; CK7, cytokeratin 7; GAPDH, glyceraldehyde 3-phosphate dehydrogenase; hEECs, human endometrial epithelial cells; IHC, immunohistochemical; IL-17, interleukin 17; OD, optical density; si-NC, negative control siRNA; si-SFRP4, siRNA targeting SFRP4.

* Corresponding author. Department of Gynecology, Women's Hospital, Zhejiang University School of Medicine, 1 Xueshi Rd, Hangzhou, 310006, China.
** Corresponding author. Department of Gynecology, Women's Hospital, Zhejiang University School of Medicine, Hangzhou, China.
E-mail address: zhoujh1117@zju.edu.cn (J. Zhou).
[1] Yunxiu Zhao and Yifei Lv contributed equally to this work and shared first authorship.
[2] Jianhong Zhou and Linjuan Ma served as corresponding authors.

https://doi.org/10.1016/j.heliyon.2024.e37168
Received 7 June 2024; Received in revised form 28 August 2024; Accepted 28 August 2024
Available online 29 August 2024

Data availability

[1]The RNAseq data have been deposited to the NCBI repository with BioProject ID PRJNA1029727. The label-free proteome data have been deposited to the ProteomeXchange Consortium via the iProX repository with the data set identifier PXD046408.

1. Introduction

The influence of abnormal uterine bleeding (AUB) among reproductive-aged women is substantial, with a global prevalence of approximately 30 % [1]. 'PALM-COEIN' has been used to categorise the causes of AUB: Polyp, Adenomyosis, Leiomyoma, Malignancy (and hyperplasia), Coagulopathy, Ovulatory disorders, Endometrial, Latrogenic, and Not otherwise classified [2,3]. AUB-O (ovulatory dysfunction) is AUB caused by anovulatory cycles and it usually involves heavy menstrual bleeding. AUB-M (atypical hyperplasia/malignancy) is AUB caused by atypical endometrial hyperplasia (AEH) or endometrial cancer (EC) [4]. The statistical comparison showed that the main cause of AUB in perimenopausal and postmenopausal patients was structural lesions, but AUB-P (27.55 %), AUB-E (21.04 %), AUB-O (18.66 %) and AUB-L (13.01 %) were the main causes in the perimenopausal group, and AUB-M (41.57 %), AUB-P (35.95 %) and AUB-M (10.11 %) in the postmenopausal group. With the increase of age, the pathogenesis of AUB gradually changes from non-structural causes such as ovulation disorder to structural factors such as AUB-M needs to be paid attention to and prevented in clinical practice. Patients with chronic AUB-O have an increased risk of EC, and the known mechanism is that ovulation disorders lead to long-term progesterone insufficiency in AUB-O patients, estrogen loses progesterone antagonism, and estrogen action makes AUB-O patients prone to endometrial hyperplasia. Therefore, the goal of AUB-O therapy is to adjust the menstrual cycle, regularity, frequency, and menstrual flow to normal and reduce the chance of EC variability, and to delay or avoid the progression of AUB-O to AUB-M [3].

In recent years, high-throughput omics analyses have become increasingly available to enhance our understanding of diseases [4]. Transcriptomic analysis focuses on coding and noncoding RNA sequences [5], producing large quantities of data on tissuessuch as endometrial tissues and peripheral blood [6]. Label-free proteomic analysis has also been used for molecular studies

Of EC and other diseases [7–9]. Transcriptomic and label-free proteomic analyses are highly complementary [10]. However, Considering the heterogeneity and complexity of AUB-O and AUB-M, such single-omics analyses may miss interactions Between different molecular entities and other biologically relevant information [11]. Althoughmulti-omic analyses have been Applied to many diseases, they have not been used to study the progression from AUB-O to AUB-M.

As a member of the secreted frizzled-related proteins (SFRP) family of glycoproteins, SFRP4 influences the canonical Wnt Signalling pathway, which regulates cell apoptosis, migration, invasion, and proliferation in various diseases [12]. The Wnt Pathway cascade is normally initiated by the binding of Wnt ligands to frizzled (Fzd) [13], which are G-coupled protein Receptors on the cell membrane [14]. Wnt-7A promotes the canonical Wnt pathway by binding to Fzd-5 [15]. However, the Detailed mechanisms underlying the progression from AUB-O to AUB-M remain to be explored. In this study, we integrated Transcriptomic and label-free proteomic data from AUB-O, AUB-M and control groups, conducted experimental validation ofthe multi-omic data and demonstrated that SFRP4 regulates the apoptosis, migration, invasion, proliferation and colony Formation abilities of hEECs.

2. Materials and methods

2.1. Endometrial tissue samples from AUB-O, AUB-M, and control participants

Endometrial tissues were obtained from the Department of Gynaecology of the Women's Hospital, School of Medicine, Zhejiang University. The informed consent was obtained for experimentation with human subjects. AUB-O (n = 9) and AUB-M (n = 9) endometrial tissues were categorised according to pathology results. Control (n = 9) endometrial samples were from women who were of similar ages to those in the AUB-O and AUB-M groups and who underwent hysteroscopy due to infertility. The control group endometrial tissues were in the proliferative endometrium. The HE staining pictures are in Fig. S5.

We conducted face-to-face interviews with the participants to obtain their demographic information, general medical history, reproductive history and menstruation information. In addition, pregnancy tests, routine blood tests (including coagulation tests) and pelvic ultrasonography were used to exclude causes of AUB that were not related to AUB-O or AUB-M. The exclusion criteria were as follows: vaginal bleeding caused by other diseases (reproductive tract trauma, genital tract foreign body, hypothyroidism and acute or chronic liver disease), immune system diseases (such as systemic lupus erythematosus), thrombotic disease, kidney dialysis, artificial heart valve replacement, history of mental illness (such as schizophrenia, moderate-to-severe depression, or neurological disorder symptoms), or taking oral antipsychotics, sex hormones, or liver enzyme inhibitors within the last 6 months. Samples were prepared as previously described by our research group [9].

2.2. Human endometrial epithelial cells (hEECs) from AUB-O participants

Endometrial tissues from AUB-O participants were centrifuged (1000g, 5 min). The precipitate was then slowly shaken at 37 °C with collagenase I (Biofroxx, China) for 1 h. The reaction was ended by adding DMEM/F12 with foetal bovine serum (FBS; BI, Israel). The homogenates were filtered through a 100-μm filter and then a 40-μm filter with phosphate-buffered saline (PBS). Finally, the 40-

μm filter was inverted and the hEECs were washed with PBS. The hEECs were cultured at 37 °C with 5 % CO_2 in DMEM/F12 added 10 % FBS.

2.3. Endometrial cancer (EC) cell lines

Ishikawa EC cells (Chinese Academy of Medical Sciences, Catalogue number CC-Y1291, Research resource identifier CVCL_2529, China), RL95-2 EC cells (Cell Bank of Chinese Academy of Sciences, Catalogue number CC-Y1637, Research resource identifier CVCL_0505, China) and Kle EC cells (American Type Culture Collection, Catalogue number BH-C213, Research resource identifier CVCL_1329, USA) were cultured in DMEM added 10 % FBS at 37 °C with 5 % CO_2.

2.4. Small interfering RNA (siRNA) transfection

SFRP4 si-RNA (si-SFRP4) and negative control siRNA (si-NC) (GenePharma, China) sequences were: SFRP4-Homo-983, 5′-CCCGCUCAUUACAAAUUCUTT-3′ (sense), 5′-AGAAUUUGUAAUGAGCGGGTT-3′ (antisense); and si-NC, 5′-UUCUCCGAACGUGUCACGUTT-3′ (sense), 5′-ACGUGACACGUUCGGAGAATT-3′ (antisense). Lipofectamine RNAiMAX (Invitrogen, USA) was used for transfection.

2.5. Transcriptomic analysis

TRIzol (Invitrogen, USA) was used for total RNA extraction. An mRNA sequencing library was prepared using 1 μg RNA with an MGIEasy RNA Directional Library Prep Kit (MGI). Differential expression analysis was done with DESeq-2 R package (v1.16.1). According to $|\log2(\text{fold change})| \geq 2.0$ with adjusted $p < 0.05$, differentially expressed genes (DEGs) were screened out. Gene Ontology (GO) and Kyoto Encyclopedia of Genes and Genomes (KEGG) were then used for further analyses.

2.6. Proteomic analysis

2.6.1. Protein digestion

The endometrial tissues were treated with lysis buffer and vortexed. After centrifugation (16,000g, 5 min, 4 °C), the supernatants were boiled, sonicated and centrifuged again (16000g, 30 min, 20 °C). The samples were prepared using FASP [16]. After being concentrated (14000g, 40 min, 20 °C) using a Microcon-30kDa Centrifugal Filter Unit (Millipore, USA), 200 μL urea buffer was added and centrifuged again (14000g, 14 min). This step was done twice. The concentrate was alkylated with iodoacetamide, centrifuged (14000g, 15 min), mixed with urea buffer for dilution and centrifuged (14000g, 15 min) again. The concentrate was then mixed with NH_4HCO_3 and centrifuged again (14000g, 15 min). Thereafter, NH_4HCO_3 and trypsin was added and placed overnight. Before peptide elution, the concentrate was washed with 40 μL 50 mM NH_4HCO_3 twice and subjected to vacuum drying. After desalting using ZipTip-C18 (Millipore, USA), the samples were dried. The precipitate concentrations were detected using 10 % acetonitrile (ACN) in 0.1 % trifluoroacetic acid (TFA).

2.6.2. Liquid chromatography (LC)-tandem mass spectrometry (MS/MS) analysis

An EASY-nLC 1000 nano-flow liquid chromatograph (Thermo Fisher Scientific, USA) was applied to separate the peptides. The LC involved buffer A and buffer B. The data were processed using Qual Browser in Xcalibur 2.2 (Thermo Fisher Scientific, USA) and searched in the UniProtKB database. The results were filtered to improve their accuracy. Differentially expressed proteins (DEPs) were defined based on $|\log2(\text{fold change})| \geq 1.0$ with adjusted $p < 0.05$. GO and KEGG were then applied for further analyses.

2.7. Cell immunofluorescence analysis

hEECs were seeded into confocal dishes (Nest, China) and allowed to reach 40%–50 % confluence. After rinsing, the hEECs were fixed with paraformaldehyde. Blocked with 1 % bovine serum albumin, the hEECs were put at 4 °C in mixture of rabbit antibody against cytokeratin 7 (ab68459; Abcam, UK) and mouse antibody against vimentin (ab20346; Abcam, UK) at dilution 1:500 over night. The hEECs were then put in goat anti-mouse secondary antibody (ab150113; Abcam, UK) mixed with goat anti-rabbit secondary antibody (ab96885; Abcam, UK) at dilution 1:500 for 1 h in the dark. Finally, DAPI was added and images were obtained with EVOS™ M5000 (ThermoFisher Invitrogen, USA).

2.8. RNA isolation and quantitative reverse transcription polymerase chain reaction (qRT-PCR)

For total RNA extraction, TRIzol was used. cDNA synthesis was performed with a PrimeScript™ RT reagent kit (TaKaRa, Japan). qRT-PCR was applied to determine SFRP4 expression with a SYBR Premix Ex Taq kit (TaKaRa, Japan). The following primer sequences obtained from PrimerBank were synthesised by Generay (Shanghai, China): SFRP4-forward: ACGAGCTGCCTGTCTATGAC, reverse: TGTCTGGTGTGATGTCTATCCAC; GAPDH-forward: GCACCGTCAAGGCTGAGAAC, reverse: TGGTGAAGACGCCAGTGGA.

2.9. Western blotting

Western blotting was conducted as previously done [17] The primary antibodies: rabbit antibody against SFRP4 at dilution 1:1000 (Invitrogen, USA), mouse antibody against GAPDH at dilution 1:10000 (Abcam, UK), rabbit antibody against SFRP2 at dilution 1:1000 (Abcam, UK), rabbit antibody against Wnt-3A at dilution 1:1000 (Cell Signaling, USA), rabbit antibody against Wnt-5A at dilution 1:500 (Abcam, UK), rabbit antibody against Wnt-7A at dilution 1:1000 (Abcam, UK), rabbit antibody against Fzd-5 at dilution 1:1000 (Abcam, UK). The secondary antibodies were anti-rabbit antibody at dilution 1:20000 (Abcam, UK) and anti-mouse antibody at dilution 1:20000 (Abcam, UK). The blots were visualised using Super ECL Detection Reagent (FDbio, China). The bands were quantified using ImageJ software.

2.10. Immunohistochemical (IHC) analysis

Endometrial tissue sections (5-μm-thick) were subjected to haematoxylin and eosin staining. The endometrial tissue sections incubated with primary rabbit antibody against SFRP4 at dilution 1:200 (ab154167, Abcam, UK) overnight at 4 °C. Then primary antibody was washed and incubated in secondary goat-anti-rabbit antibody at dilution 1:200 (Invitrogen, USA) for 1 h at 37 °C, treated with diaminobenzidine (DAB, Sigma, USA) and scanned using an Ocus® scanner (Grundium, Finland). The results were calculated as previously described [18].

2.11. Flow cytometry apoptosis assays

After 48h transfection with indicated si-RNA, 1×10^6 hEECs were incubated in 1 × binding buffer with annexin V-APC and 7-AAD (MULTI SCIENCES, China) with light avoidance for 5 min and analysed by flow cytometry.

2.12. Terminal deoxyribonucleotide transferase (TdT)-mediated dUTP nick end labelling (TUNEL) apoptosis assays

After 72h transfection with indicated si-RNA, 1×10^6 hEECs were mixed with paraformaldehyde, permeabilised using 0.3 % Triton X-100 (Biosharp, China), washed with PBS, mixed with TUNEL mixture (Beyotime, China), incubated at 37 °C for 1 h with light avoidance and imaged using EVOS™ M5000 (ThermoFisher Invitrogen, USA).

2.13. Transwell migration and invasion assays

Transwell assays were conducted as previously done [19]. Briefly, transwell chambers and polycarbonate filters (pore size, 8 mm) (Corning, USA) were used. After 48 h transfection with si-SFRP4 or si-NC, 5×10^5 (migration) or 1×10^6 (invasion) hEECs in 200 μl DMEM was put into the upper chamber, while 500 μl DMEM added 10 % FBS was put into the lower chamber. In contrast to the migration assays, the invasion assays involved the addition of Matrigel (BD Biosciences, USA). After 24 h or 48 h, the crystal violet stained hEECs were imaged by EVOS™ M5000 (ThermoFisher Invitrogen, USA) under a 20× magnification microscope. Three separate fields were randomly captured for each chamber. The number of hEECs in each field was counted with ImageJ software.

2.14. Wound healing assays

In the wound healing assays, hEECs in 6 well plates were allowed to reach >95 % confluence. After 48 h transfection with indicated si-RNA, wounds were made. The width of each wound was photographed under a 10× magnification phase-contrast microscope at 0 and 12 h using EVOS™ M5000 (ThermoFisher Invitrogen, USA). Percentage of wound healing was calculated as previously described [20].

2.15. Cell counting Kit-8 (CCK-8) assays

5×10^3 hEECs/well (100 μl hEECs suspension) in 96 well plates were incubated at 37 °C with 5 % CO_2 for 24 h. After 48 h indicated si-RNA transfection, the medium was replaced with 100 μl CCK-8 reagent (Beyotime, China) in DMEM/well (1:9) and incubated in the dark for 3 h. Each sample was conducted 5 replicates. The 450 nm optical density (OD) value was calculated every 24 h for 5 days.

2.16. EdU staining assays

In the EdU staining assays, 3.5×10^4 hEECs/well in 24-well plates were placed overnight. After 48 h transfection with indicated si-RNA, BeyoClick™ EdU-594 (Beyotime, China) was added to detect the EdU incorporation rate. The EdU-labeled rate was determined by the ratio of EdU-labeled (red) to DAPI-labeled cells (blue). Pictures were imaged by EVOS™ M5000 (ThermoFisher Invitrogen, USA).

2.17. Colony formation assays

In the colony formation assays, 2×10^3 hEECs/well were placed into 6-well plates and placed overnight. After transfection with

indicated si-RNA, the cells were incubated for 14 days. Finally, the crystal violet stained hEECs colonies were imaged and counted.

2.18. Statistical analyses

Most of the bioinformatics analyses were conducted as outlined above. The statistical analyses were done with SPSS 24.0 and R 3.6.3. The data are presented as mean ± standard deviation, median (Q1, Q3), or frequency (percentage). Fisher's exact test, analysis of variance (ANOVA), the chi-square test, and Kruskal–Wallis test were also used. $p < 0.05$ was considered statistically significant.

3. Results

3.1. Participant characteristics

The participant characteristics are presented in Table S1. The median age was 29 (26, 31), 30 (27, 36) and 38 (37, 40) in the control, AUB-O and AUB-M groups, respectively ($p = 0.001$). The mean body mass index was 21.3 ± 2.2, 20.9 ± 3.4 and 25.1 ± 2.8 kg/m^2, respectively ($p = 0.008$). There were 2 (7.4 %), 7 (25.9 %) and 9 (33.3 %) participants in the control,

AUB-O and AUB-M groups, respectively, that lived in the countryside ($p = 0.002$). Education level and occupation significantly differed among the three groups ($p = 0.018$, $p = 0.00002$). There were no significant differences in age at menarche (days), menstruation duration (days), menstrual cycle length (days), haemoglobin (g/L), luteinising hormone (IU/L), E2 (pmol/L), progesterone (ng/ml), testosterone (ng/ml), thyroid-stimulating hormone (mI/L), free T3 (pg/L), free T4 (pg/L), or anti-thyroid peroxidase antibody (IU/ml) (all $p > 0.05$).

3.2. DEGs

There were 828 DEGs (236 upregulated and 592 downregulated) for control vs. AUB-M and 48 DEGs (26 upregulated and 22 downregulated) for control vs. AUB-O (Figs. S1A and S2A). Tables S2 and S3 show the GO and KEGG analyses of these DEGs.

There were 786 DEGs (223 upregulated and 563 downregulated) for AUB-O vs. AUB-M (Fig. 1A). Table 1 shows the GO and KEGG analyses of these DEGs. Of the 143 significantly enriched GO Biological Process (BP) terms, the top terms were axoneme assembly, cilium movement, microtubule bundle formation, cilium or flagellum-dependent cell motility and

Cilium-dependent cell motility. Of the 118 significantly enriched GO Cellular Component (CC) terms, the top terms were motile cilium, axoneme, ciliary plasm, 9 + 2 motile cilium and axonemal dynein complex. Of the 47 significantly enriched GO Molecular Function (MF) terms, the top terms were minus-end-directed microtubule motor activity, CXCR chemokine receptor binding, chemokine activity, insulin-like growth factor binding and cytokine activity. Of the 57 significantly enriched KEGG pathways, the top pathways were rheumatoid arthritis, interleukin (IL)-17 signalling pathway, glutamatergic synapse, viral protein interaction with cytokine and cytokine receptor and legionellosis.

3.3. DEPs

There were 74 DEPs (21 upregulated and 53 downregulated) for control vs. AUB-M and 30 DEPs (9 upregulated and 21 downregulated) for control vs. AUB-O (Figs. S1B and S2B). GO and KEGG analyses of these DEPs are shown in Tables S4 and S5.

There were 79 DEPs (8 upregulated and 71 downregulated) for AUB-O vs. AUB-M (Fig. 1B). Table 2 shows the GO and KEGG analyses of these DEPs. Of the 13 significantly enriched GO BP terms, the top terms were homotypic cell–cell adhesion, regulation of cardiac muscle cell action potential, negative regulation of fibroblast proliferation, regulation of membrane potential and positive regulation of epithelial cell apoptotic process. Of the 10 significantly enriched GO MF terms, the top terms were calcium-dependent protein binding, ion channel regulator activity, channel regulator activity, chloride channel inhibitor activity and transcription coregulator activity. There were no significantly enriched GO CC terms for the DEPs.

3.4. Integrative multi-omic analyses

Volcano plots indicated that the DEGs and DEPs could clearly distinguish between any two groups, i.e. control vs. AUB-M, control vs. AUB-O and AUB-O vs. AUB-M (Fig. S1C–D, S2C–D and 1C–D, respectively). The top GO and KEGG terms of DEGs and DEPs are shown in Fig. S1E–H, S2E–H and 1E–H, respectively.

Venn diagrams of the DEGs and DEPs showed that only one molecule (SFRP4) was simultaneously changed in the transcriptomic and proteomic analyses between AUB-O and AUB-M (Fig. S1I, S2I and 1I).

3.5. Validation of SFRP4 biomarker in endometrial tissues

SFRP4 expression in endometrial tissues was confirmed to significantly differ between the AUB-O and AUB-M (AEH and EC) groups (all $p < 0.05$) by qRT-PCR (n = 3), western blotting (n = 3) and IHC (n = 4) (Fig. 2A–D). There were consistent differences in the transcriptomic and proteomic datasets, with SFRP4 always being upregulated in the AUB-O group compared to the AUB-M group.

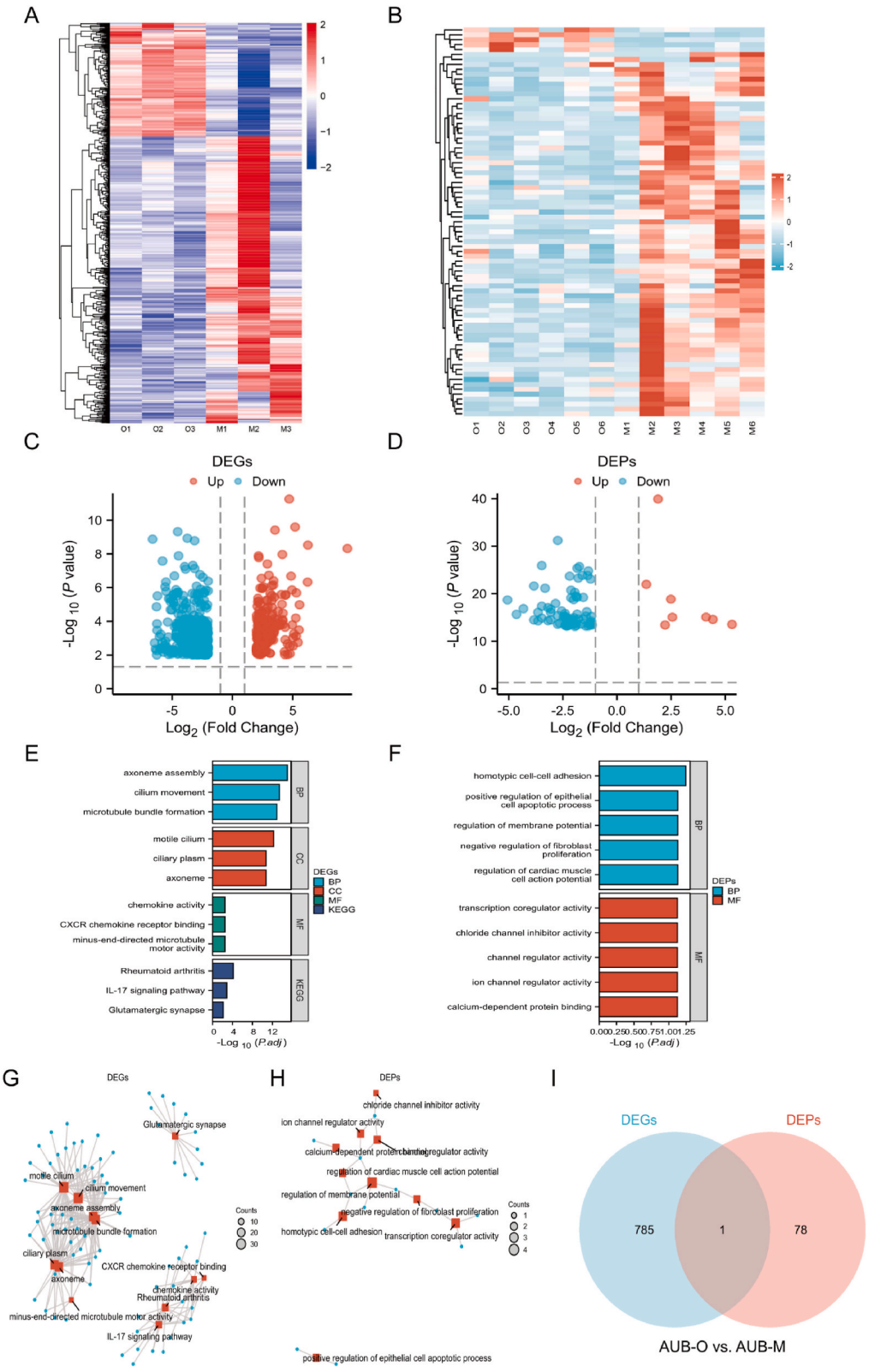

(caption on next page)

Fig. 1. Integrated analyses of transcriptomic and proteomic data between abnormal uterine bleeding with ovulatory dysfunction (AUB-O) and abnormal uterine bleeding with atypical hyperplasia/malignancy (AUB-M) groups. (A) Heatmap of hierarchical clustering analysis of DEGs between the two groups. (B) Heatmap of hierarchical clustering analysis of DEPs between the two groups. (C) Volcano plot of molecules in the two groups based on transcriptomic data. (D) Volcano plot of molecules in the two groups based on proteomic data. (E and G) Top GO and KEGG terms of DEGs between the two groups. (F and H) Top GO and KEGG terms of DEPs between the two groups. (I) Venn diagram of DEGs and DEPs between the two groups. AUB-O groups: O1-O6; AUB-M groups: M1-M6.

Table 1
GO and KEGG enrichment analyses of DEGs between AUB-O and AUB-M groups.

Ontology	ID	Description	GeneRatio	BgRatio	*p*value	*p*.adjust
BP	GO:0035082	axoneme assembly	26/560	87/18800	2.25e-19	9.46e-16
BP	GO:0003341	cilium movement	34/560	187/18800	1.71e-17	3.58e-14
BP	GO:0001578	microtubule bundle formation	27/560	118/18800	8.62e-17	1.21e-13
BP	GO:0001539	cilium or flagellum-dependent cell motility	28/560	151/18800	7.37e-15	6.18e-12
BP	GO:0060285	cilium-dependent cell motility	28/560	151/18800	7.37e-15	6.18e-12
CC	GO:0031514	motile cilium	35/585	227/19594	1.31e-15	5.04e-13
CC	GO:0005930	axoneme	25/585	131/19594	1.12e-13	1.73e-11
CC	GO:0097014	ciliary plasm	25/585	132/19594	1.35e-13	1.73e-11
CC	GO:0097729	9 + 2 motile cilium	23/585	149/19594	1.02e-10	9.8e-09
CC	GO:0005858	axonemal dynein complex	10/585	23/19594	4.2e-10	3.24e-08
MF	GO:0008569	minus-end-directed microtubule motor activity	6/563	18/18410	1.08e-05	0.0033
MF	GO:0045236	CXCR chemokine receptor binding	6/563	18/18410	1.08e-05	0.0033
MF	GO:0008009	chemokine activity	9/563	49/18410	1.51e-05	0.0033
MF	GO:0005520	insulin-like growth factor binding	7/563	29/18410	2.09e-05	0.0035
MF	GO:0005125	cytokine activity	19/563	235/18410	0.0001	0.0108
KEGG	hsa05323	Rheumatoid arthritis	14/228	93/8164	2.47e-07	6.57e-05
KEGG	hsa04657	IL-17 signaling pathway	12/228	94/8164	1.06e-05	0.0014
KEGG	hsa04724	Glutamatergic synapse	12/228	114/8164	7.52e-05	0.0067
KEGG	hsa04061	Viral protein interaction with cytokine and cytokine receptor	11/228	100/8164	0.0001	0.0067
KEGG	hsa05134	Legionellosis	8/228	57/8164	0.0002	0.0088

Table 2
GO and KEGG enrichment analyses of DEPs between AUB-O and AUB-M groups.

Ontology	ID	Description	GeneRatio	BgRatio	*p*value	*p*.adjust
BP	GO:0034109	homotypic cell-cell adhesion	3/17	93/18800	7.58e-05	0.0572
BP	GO:0098901	regulation of cardiac muscle cell action potential	2/17	28/18800	0.0003	0.0740
BP	GO:0048147	negative regulation of fibroblast proliferation	2/17	30/18800	0.0003	0.0740
BP	GO:0042391	regulation of membrane potential	4/17	425/18800	0.0005	0.0740
BP	GO:1904037	positive regulation of epithelial cell apoptotic process	2/17	38/18800	0.0005	0.0740
MF	GO:0048306	calcium-dependent protein binding	2/17	87/18410	0.0029	0.0750
MF	GO:0099106	ion channel regulator activity	2/17	138/18410	0.0070	0.0750
MF	GO:0016247	channel regulator activity	2/17	143/18410	0.0075	0.0750
MF	GO:0019869	chloride channel inhibitor activity	1/17	10/18410	0.0092	0.0750
MF	GO:0003712	transcription coregulator activity	3/17	497/18410	0.0100	0.0750

3.6. Validation of SFRP4 biomarker in human endometrial epithelial cells (hEECs)

CK7 positivity and vimentin negativity of hEECs (from AUB-O patients) was confirmed by cell immunofluorescence analysis (Fig. 3A). In cultured hEECs, SFRP4 was expressed predominantly in nuclei but also in cytoplasm, but mainly found in the cell cytoplasm (Fig. 3C). qRT-PCR and western blotting showed that SFRP4 was upregulated in hEECs (from AUB-O patients) (n = 3) compared to Ishikawa, Kle and RL95-2 EC cells (n = 3) (all $p < 0.05$, Fig. 3B and D).

3.7. SFRP4 knockdown inhibited apoptosis

We transfected hEECs with si-SFRP4 or si-NC. The knockdown efficiency of si-SFRP4 was confirmed by western blotting (Fig. 4A) and qRT-PCR (Fig. S3). Then we performed flow cytometry and TUNEL on hEECs transfected with si-SFRP4 or si-NC. SFRP4 knockdown reduced apoptosis ($p < 0.05$, Fig. 4B and C).

3.8. SFRP4 knockdown promoted hEECs migration, invasion and proliferation

Thereafter, we performed transwell, wound healing, CCK-8, EdU staining and colony formation assays on hEECs transfected with si-SFRP4 or si-NC. SFRP4 knockdown increased hEECs migration, invasion abilities (all $p < 0.05$, Fig. 5A and B). The traditional study of

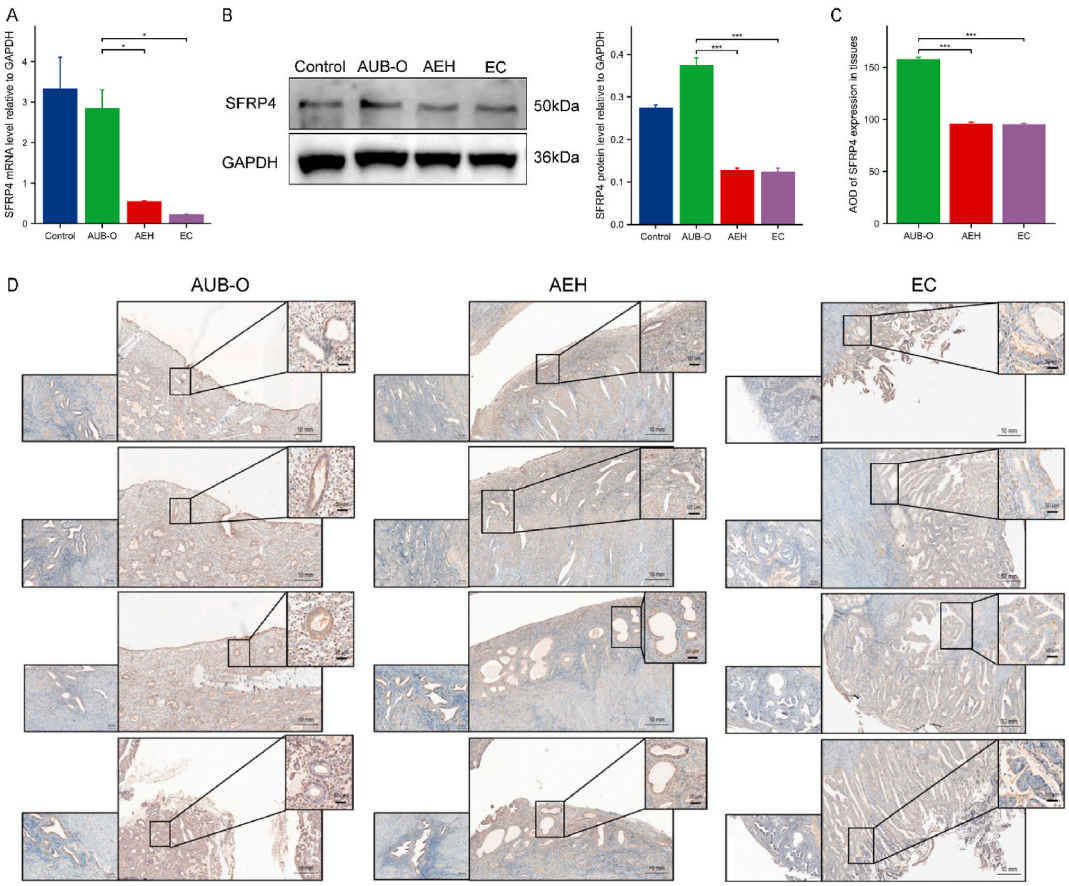

Fig. 2. Secreted frizzled-related protein 4 (SFRP4) expression in control, AUB-O, AUB with atypical hyperplasia (AEH) and AUB with endometrial cancer (EC) groups of endometrial tissues based on quantitative reverse transcription polymerase chain reaction (qRT-PCR), western blotting and immunohistochemical (IHC) analysis. (A) SFRP4 mRNA levels in the four groups of endometrial tissues based on qRT-PCR (n = 3). (B) SFRP4 protein levels in the four groups of endometrial tissues based on western blotting (n = 3). For the uncropped versions of western blotting, please refer to Supplement Files. (C–D) SFRP4 protein levels in endometrial tissues of the AUB-O, AEH and EC groups based on IHC analysis (n = 4). Negative control is shown in the lower-left rectangles (magnification, × 100). GAPDH, glyceraldehyde-3-phosphate dehydrogenase. Data are presented as mean ± SD. *$p < 0.05$; ***$p < 0.001$.

Wnt signalling in tumorigenesis has mainly focused on the effects of Wnt signalling hyperactivation on cell proliferation, which are mainly due to β-catenin-mediated transcriptional activation of Cyclin D1, which promotes cell proliferation. We performed western blotting in endometrial tissues, hEECs, and Ishikawa cells ($p < 0.05$, Fig. 6A). SFRP4 knockdown increased hEECs proliferation and colony formation abilities (all $p < 0.05$, Fig. 6B–D).

3.9. SFRP4 knockdown influenced the Wnt pathway in hEECs

To explore the effect of SFRP4 on the Wnt pathway in hEECs, the expression levels of several key factors in the Wnt pathway were determined by western blotting (Fig. 7A and B). Our findings indicated that SFRP4 knockdown in hEECs downregulated Wnt-5A and upregulated Wnt-7A. The protein expression of Wnt-3A, Wnt-5A and Wnt-7A in the AUB-O and AUB-M patients were in Fig. S4.

4. Discussion

In some countries, particularly (but not limited to) the United States, ovulatory disorders comprise the vast majority of AUB cases. These ovulatory disorders may present as a spectrum of menstrual abnormalities, and extremely heavy menstrual bleeding requires medical or surgical intervention [21]. AUB-M caused by EC and AEH accounts for 1%–2% of cases involving premenopausal women with AUB; endometrial function (in terms of menstruation and menstruation disorders) has not yet been fully explored in AUB-M patients [22]. Transcriptomic and proteomic analyses have been used to reveal the mechanisms of various diseases, including AUB-M [23–25]. However, there has been no omics research on the mechanisms underlying how AUB-O develops into AUB-M. As a single-omics analysis can miss important crosstalk between different molecular patterns and other biologically significant information [11], we conducted comprehensive integrative transcriptomic and label-free proteomic analyses in order to reveal the pathological

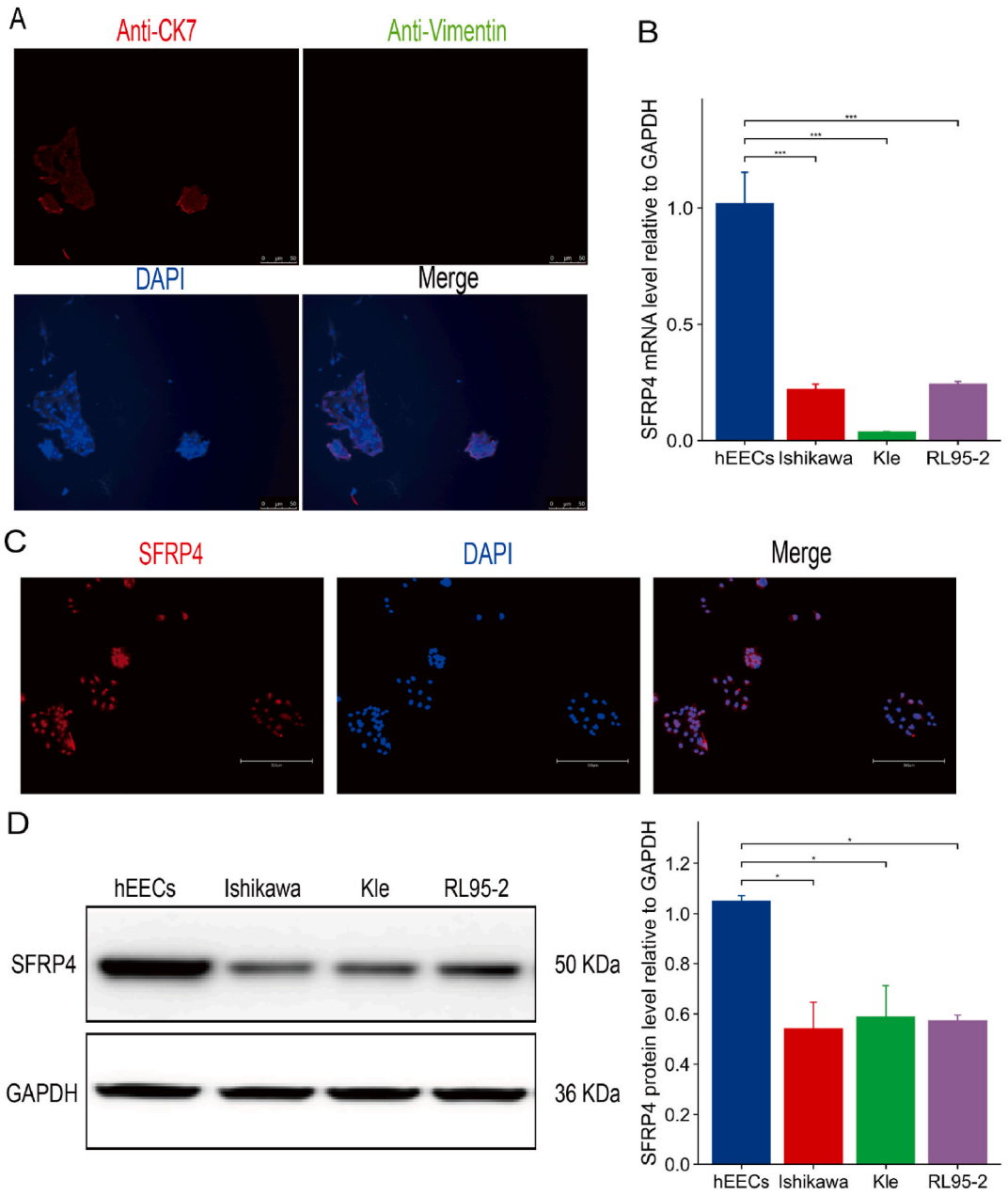

Fig. 3. Morphological identification of human endometrial epithelial cells (hEECs) based on cell immunofluorescence analysis and SFRP4 expression in hEECs and endometrial cancer (EC) cells. (A) Morphology of hEECs based on cell immunofluorescence analysis (magnification, × 20; CK7 positive: red, vimentin positive: green). (B) SFRP4 mRNA levels in hEECs, Ishikawa, Kle and RL95-2 cells based on qRT-PCR (n = 3). (C) The immunofluorescent detection of SFRP4 in the hEECs. (D) SFRP4 protein levels in hEECs, Ishikawa, Kle and RL95-2 cells based on western blotting (n = 3). For the uncropped versions of western blotting, please refer to Supplement Files. Data are presented as mean ± SD. *$p < 0.05$; ***$p < 0.001$.

changes involved in the progression of AUB-O to AUB-M, and we identified a single biomarker: SFRP4.

GO and KEGG analysis demonstrated that DEPs were enriched in the positive regulation of epithelial apoptosis between AUB-O group and AUB-M group, and DEGs and ciliary motility were enriched between AUB-O group and AUB-M group, suggesting that differentially expressed proteins and differentially expressed genes were enriched in cell function in apoptosis and cell motility. Therefore, we consider that the molecular mechanism of AUB-O progression to AUB-M may be related to apoptosis, motility, and proliferation.

SFRP4 is known to serve as a biomarker in cancers such as cervical cancer, ovarian cancer and mesothelioma [26]. SFRP4 was reported to be downregulated in EC compared to normal endometrial tissues, while stable SFRP4 overexpression in vitro inhibited colony formation by EC cells [15]. However, little was known about SFRP4 in hEECs from AUB-O patients. Based on our results, we

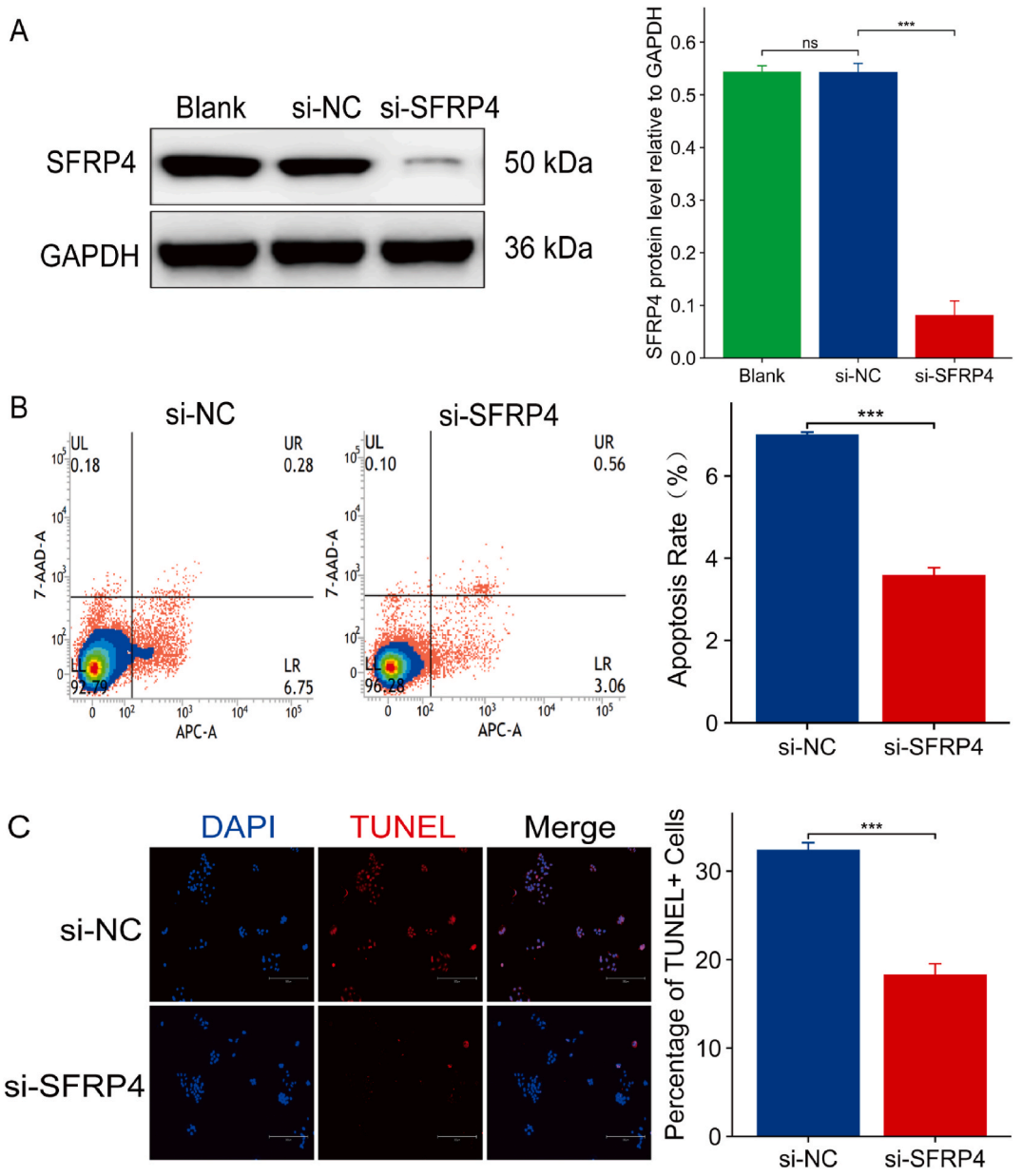

Fig. 4. Effects of SFRP4 knockdown in hEECs on apoptosis. (A) SFRP4 knockdown efficiency in hEECs based on western blotting 72 h after si-NC and si-SFRP4 treatment (n = 3). For the uncropped versions of western blotting, please refer to Supplement Files. (B) Flow cytometry assays of apoptosis (n = 3). (C) TUNEL staining assays of apoptosis (n = 3). Data are presented as mean ± SD. ns, no significance; ***$p < 0.001$.

hypothesise that SFRP4 plays an essential repressive role regarding the progression from AUB-O to AUB-M. SFRP4 mRNA and protein expression levels were examined in AUB-O, AUB-M (AEH and EC) and control endometrial tissues, and SFRP4 was found to be upregulated in AUB-O compared to AUB-M. We isolated hEECs with CK7 positivity and vimentin negativity (based on cell immunofluorescence analysis), which are characteristics of hEECs in the endometrium [27]. We then demonstrated that SFRP4 knockdown in hEECs promoted cell migration, invasion, proliferation and colony formation but suppressed apoptosis. All in all, these results suggest that SFRP4 may serve as a repressive factor regarding the progression of AUB-O into AUB-M.

Secreted frizzled-related protein 2 (SFRP2), which is a member of the SFRP family, has been reported to be a negative modulator of canonical Wnt signalling [28]. However, the association of SFRP2 with SFRP4 remains to be explored. SFRP4, which has a similar sequence to the extracellular domain of Fzd [29], not only interacts with Wnt proteins to prevent them from binding to Fzd [30], but also activates Wnt signalling under certain conditions [15]. However, how SFRP4 influences the protein expression of Wnt and Fzd has not been researched. Our findings indicated that SFRP4 knockdown in hEECs using si-SFRP4 downregulated Wnt-5A protein and upregulated Wnt-7A protein. Therefore, we speculate that si-SFRP4 may alter the phenotype from AUB-O to AUB-M by influencing

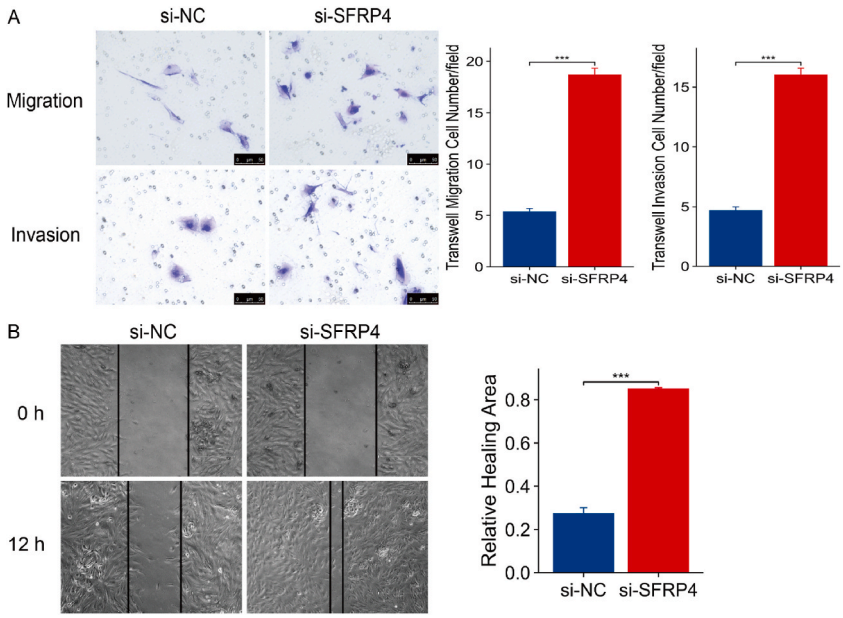

Fig. 5. Effects of SFRP4 knockdown in hEECs on migration, invasion and proliferation. (A) Transwell assays of migration and invasion (magnification, × 20) (n = 3). (B) Wound healing assays of migration (magnification, × 10) (n = 3). (C) Cell counting kit-8 assays of proliferation (n = 3). (D) EdU staining assays of proliferation (n = 3). (E) Colony formation assays of proliferation (n = 3). Data are presented as mean ± SD. ns, no significance; $^{**}p < 0.01$; $^{***}p < 0.001$.

Wnt-5A and Wnt-7A.

The limitations of this study should be kept in mind. The samples of AUB-O (n = 9) and AUB-M (n = 9) patients were relatively small; a larger study should be conducted to further investigate the diagnostic efficacy of SFRP4. Additionally,

In-depth studies are required to identify the detailed mechanism underlying the progression of AUB-O to AUB-M.

In summary, given the prevalence of AUB-O and AUB-M, there is an urgent need to understand how AUB-O develops into AUB-M in order to offer optimal individualised diagnosis and treatment for patients. In this study, transcriptomic and

Label-free proteomic analyses were used to compare human endometrium tissues among AUB-O, AUB-M and control groups. SFRP4 was upregulated in AUB-O endometrial tissues compared to AUB-M endometrial tissues according to qRT-PCR, western blotting and IHC analysis. Moreover, we demonstrated that SFRP4 knockdown promoted hEEC migration, invasion, proliferation and colony formation via the Wnt pathway. Although there were limitations, this study provides up-to-date information on the potential repressive mechanism involving SFRP4 regarding the progression of AUB-O into AUB-M, which is key for the advancement of women's health-related quality of life.

Consent for publication

All data have consent for publication.

Funding

This work was supported by the National Key Research and Development Program of China [grant number 2022YFC2704101].

This work was supported by the Science and Technology Program of Zhejiang Province, China [grant number 2019C03026].

This work was supported by 4+X Clinical Research Project of Women's Hospital, School of Medicine, Zhejiang University [grant number ZDFY2023-4X201].

Ethics approval and consent to participate

This work was reviewed and approved by the Ethics Committee of Women's Hospital, School of Medicine, Zhejiang University located in Hangzhou, Zhejiang Province, China with the Ethical Clearance (No. 20180200). Informed consent was obtained from all subjects.

CRediT authorship contribution statement

Yunxiu Zhao: Writing – original draft, Visualization, Validation, Software, Methodology, Investigation, Formal analysis, Data

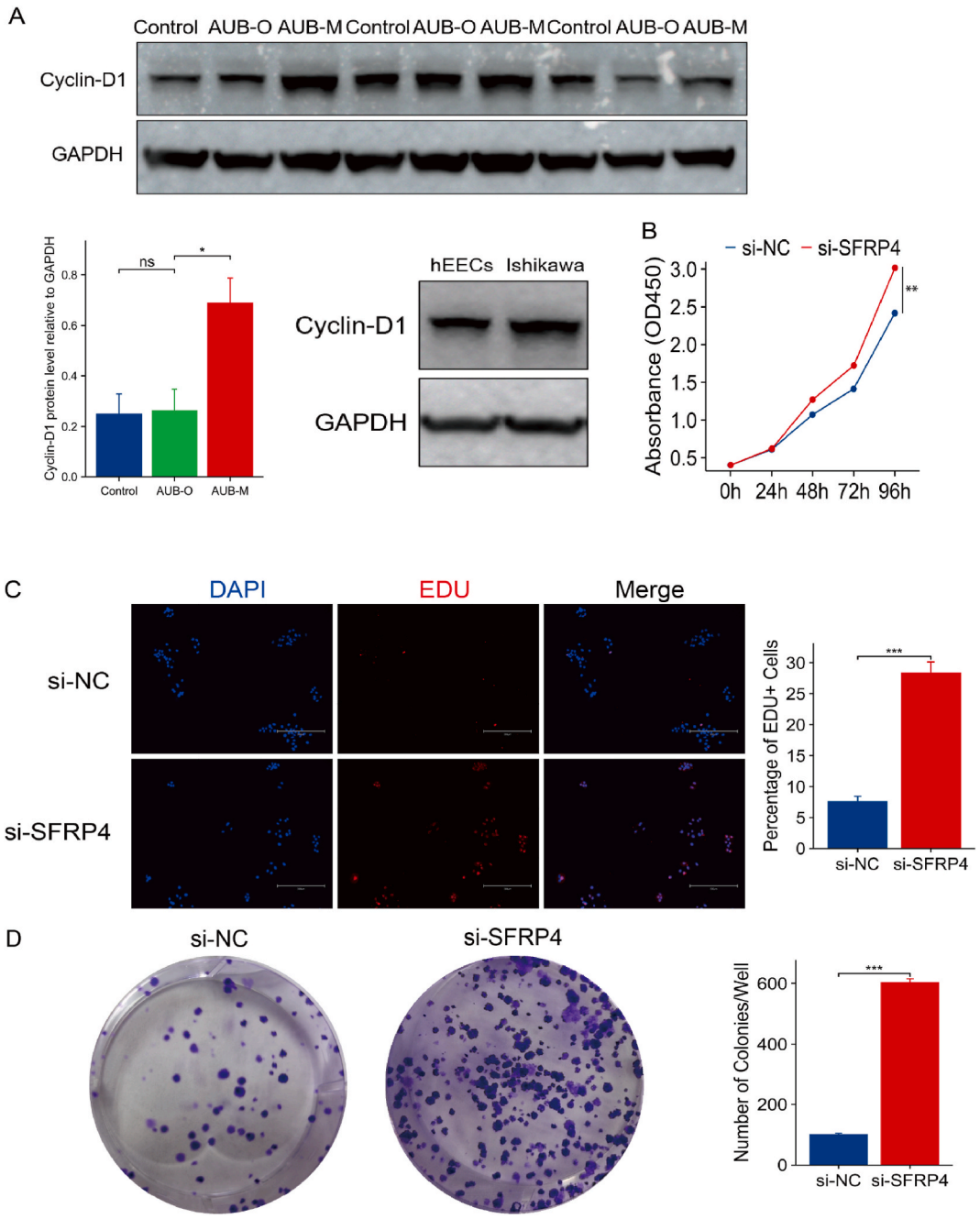

Fig. 6. Effects of SFRP4 knockdown in hEECs on proliferation. (A) The protein expression of cyclin D1 in control, AUB-O and AUB-M endometrial tissues (n = 4). The protein expression of cyclin D1 in isolated hEECs of AUB-O and Ishikawa cells (n = 4). For the uncropped versions of western blotting, please refer to Supplement Files. (B) Cell counting kit-8 assays of proliferation (n = 3). (C) EdU staining assays of proliferation (n = 3). (D) Colony formation assays of proliferation (n = 3). Data are presented as mean ± SD. ns, no significance; *$p < 0.05$; **$p < 0.01$; ***$p < 0.001$.

curation, Conceptualization. **Yifei Lv:** Software, Methodology, Formal analysis, Data curation. **Yizhou Huang:** Validation, Software. **Tao Zhang:** Data curation. **Yibing Lan:** Methodology. **Chunming Li:** Software. **Peiqiong Chen:** Project administration. **Wenxian Xu:** Formal analysis. **Linjuan Ma:** Writing – review & editing, Project administration, Funding acquisition, Data curation. **Jianhong Zhou:** Writing – review & editing, Supervision, Resources, Project administration, Funding acquisition.

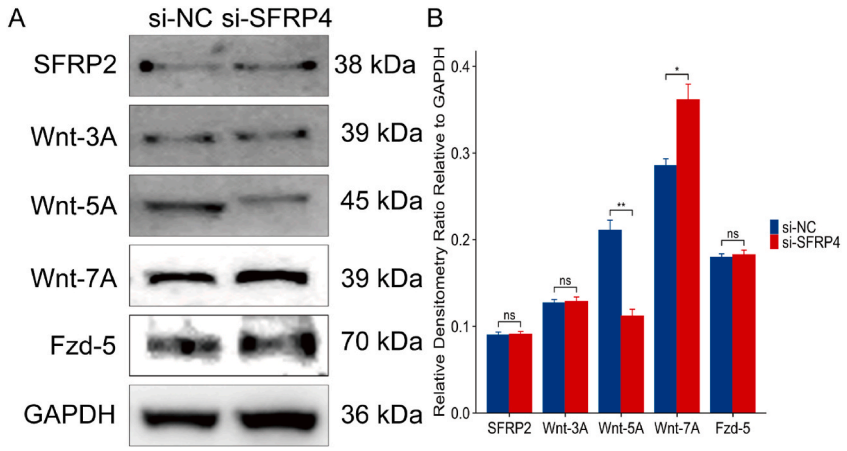

Fig. 7. Effects of SFRP4 knockdown in hEECs on the Wnt pathway. Expression of SFRP2, Wnt-3A, Wnt-5A, Wnt-7A and Fzd-5 was measured in hEECs transfected with si-NC or si-SFRP4 by western blotting 72 h later. (A) Representative western blots of SFRP2, Wnt-3A, Wnt-5A, Wnt-7A and Fzd-5 in the si-NC and si-SFRP4 groups (n = 4). For the uncropped versions of western blotting, please refer to Supplement Files. (B) Relative densitometric values of SFRP2, Wnt-3A, Wnt-5A, Wnt-7A and Fzd-5 in the si-NC and si-SFRP4 groups. Data are presented as mean ± SD. ns, no significance; *$p < 0.05$; **$p < 0.01$.

Declaration of competing interest

The authors declare that they have no known competing financial interests or personal relationships that could have appeared to influence the work reported in this paper.

Acknowledgments

We thank the patients who agreed to take part in this study. Acknowledgments also go to professors who provided help.

Appendix A. Supplementary data

Supplementary data to this article can be found online at https://doi.org/10.1016/j.heliyon.2024.e37168.

References

[1] R.A. Werneck, M.F. Meinberg, M.Z. Passos, W.C. Brandão, E.N. de Moraes, A.L. da Silva-Filho, Quality of information regarding abnormal uterine bleeding available online, Eur. J. Obstet. Gynecol. Reprod. Biol. 282 (2023) 83–88.
[2] M.G. Munro, H.O. Critchley, I.S. Fraser, The FIGO systems for nomenclature and classification of causes of abnormal uterine bleeding in the reproductive years: who needs them? Am. J. Obstet. Gynecol. 207 (2012) 259–265.
[3] C.L. Benetti-Pinto, A.C.J.S. Rosa-E-Silva, D.A. Yela, J.M. Soares Júnior, Abnormal uterine bleeding. Sangramento uterino anormal, Rev. Bras. Ginecol. Obstet. 39 (7) (2017) 358–368, https://doi.org/10.1055/s-0037-1603807.
[4] K. Njoku, C.J. Sutton, A.D. Whetton, E.J. Crosbie, Metabolomic biomarkers for detection, prognosis and identifying recurrence in endometrial cancer, Metabolites 10 (2020) 314.
[5] X. Hu, C. Tao, Q. Gan, J. Zheng, H. Li, C. You, Oxidative stress in intracerebral hemorrhage: sources, mechanisms, and therapeutic targets, Oxid. Med. Cell. Longev. 2016 (2016) 3215391.
[6] M. Raliou, D. Dembélé, A. Düvel, P. Bolifraud, J. Aubert, T. Mary-Huard, D. Rocha, F. Piumi, S. Mockly, M. Heppelmann, I. Dieuzy-Labaye, P. Zieger, D.G. E. Smith, H.J. Schuberth, I.M. Sheldon, O. Sandra, Subclinical endometritis in dairy cattle is associated with distinct mRNA expression patterns in blood and endometrium, PLoS One 14 (2019) e0220244.
[7] U. Distler, J. Kuharev, S. Tenzer, Biomedical applications of ion mobility-enhanced data-independent acquisition-based label-free quantitative proteomics, Expert Rev. Proteomics 11 (2014) 675–684.
[8] S.S. Gautam, R.P. Singh, K. Karsauliya, A.K. Sonker, P.J. Reddy, D. Mehrotra, S. Gupta, S. Singh, R. Kumar, S.P. Singh, Label-free plasma proteomics for the identification of the putative biomarkers of oral squamous cell carcinoma, J. Proteonomics 259 (2022) 104541.
[9] Y. Jia, J. Luo, Y. Lan, C. Li, L. Ma, X. Zhu, F. Ruan, J. Zhou, Label-free proteomics uncovers SMC1A expression is down-regulated in AUB-E, Reprod. Biol. Endocrinol. 19 (2021) 35.
[10] S. Artigaud, J. Richard, M.A. Thorne, R. Lavaud, J. Flye-Sainte-Marie, F. Jean, L.S. Peck, M.S. Clark, V. Pichereau, Deciphering the molecular adaptation of the king scallop (*Pecten maximus*) to heat stress using transcriptomics and proteomics, BMC Genom. 16 (2015) 988.
[11] J. Montaner, L. Ramiro, A. Simats, S. Tiedt, K. Makris, G.C. Jickling, S. Debette, J.C. Sanchez, A. Bustamante, Multilevel omics for the discovery of biomarkers and therapeutic targets for stroke, Nat. Rev. Neurol. 16 (2020) 247–264.
[12] C. Chen, Q. Zhang, B. Kong, miRNA-576-5p promotes endometrial cancer cell growth and metastasis by targeting ZBTB4, Clin. Transl. Oncol. 25 (2022) 706–720.
[13] T. Constantinou, F. Baumann, M.D. Lacher, S. Saurer, R. Friis, A. Dharmarajan, SFRP-4 abrogates Wnt-3a-induced β-catenin and Akt/PKB signalling and reverses a Wnt-3a-imposed inhibition of in vitro mammary differentiation, J. Mol. Signal. 3 (2008) 10.

[14] H.Y. Wang, C.C. Malbon, Wnt-frizzled signaling to G-protein-coupled effectors, Cell. Mol. Life Sci. 61 (2004) 69–75.
[15] K.S. Carmon, D.S. Loose, Secreted frizzled-related protein 4 regulates two Wnt 7A signaling pathways and inhibits proliferation in endometrial cancer cells, Mol. Cancer Res. 6 (2008) 1017–1028.
[16] J.R. Wiśniewski, N. Nagaraj, A. Zougman, F. Gnad, M. Mann, Brain phosphoproteome obtained by a FASP-based method reveals plasma membrane protein topology, J. Proteome Res. 9 (2010) 3280–3289.
[17] H. Zhan, J. Ma, F. Ruan, M.A. Bedaiwy, B. Peng, R. Wu, J. Lin, Elevated phosphatase of regenerating liver 3 (PRL-3) promotes cytoskeleton reorganization, cell migration and invasion in endometrial stromal cells from endometrioma, Hum. Reprod. 31 (2016) 723–733.
[18] Y. Wang, C. Wu, Y. Qin, S. Liu, R. Zhang, Multi-angle investigation of the fractal characteristics of nanoscale pores in the lower Cambrian Niutitang shale and their implications for CH_4 adsorption, J. Nanosci. Nanotechnol. 21 (2021) 156–167.
[19] Y. Lv, L. Zhang, J. Ma, X. Fei, K. Xu, J. Lin, CTHRC1 overexpression promotes ectopic endometrial stromal cell proliferation, migration and invasion via activation of the Wnt/β-catenin pathway, Reprod. Biomed. Online 40 (2020) 26–32.
[20] K.H. Song, M.S. Park, T.S. Nandu, S. Gadad, S.C. Kim, M.Y. Kim, GALNT14 promotes lung-specific breast cancer metastasis by modulating self-renewal and interaction with the lung microenvironment, Nat. Commun. 7 (2016) 13796.
[21] G.E. Hale, C.L. Hughes, H.G. Burger, D.M. Robertson, I.S. Fraser, Atypical estradiol secretion and ovulation patterns caused by luteal out-of-phase (LOOP) events underlying irregular ovulatory menstrual cycles in the menopausal transition, Menopause 16 (2009) 50–59.
[22] M.A. Clarke, B.J. Long, A. Del Mar Morillo, M. Arbyn, J.N. Bakkum-Gamez, N. Wentzensen, Association of endometrial cancer risk with postmenopausal bleeding in women: a systematic review and meta-analysis, JAMA Intern. Med. 178 (2018) 1210–1222.
[23] M.A. Kodura, S. Souchelnytskyi, Breast carcinoma metastasis suppressor gene 1 (BRMS1): update on its role as the suppressor of cancer metastases, Cancer Metastasis Rev. 34 (2015) 611–618.
[24] P.S. Steeg, Targeting metastasis, Nat. Rev. Cancer 16 (2016) 201–218.
[25] C.H. Stuelten, C.A. Parent, D.J. Montell, Cell motility in cancer invasion and metastasis: insights from simple model organisms, Nat. Rev. Cancer 18 (2018) 296–312.
[26] S. Pohl, R. Scott, F. Arfuso, V. Perumal, A. Dharmarajan, Secreted frizzled-related protein 4 and its implications in cancer and apoptosis, Tumour Biol 36 (2015) 143–152.
[27] F. Ramaekers, A. Huysmans, G. Schaart, O. Moesker, P. Vooijs, Tissue distribution of keratin 7 as monitored by a monoclonal antibody, Exp. Cell Res. 170 (1987) 235–249.
[28] J. Ren, F. Jian, H. Jiang, Y. Sun, S. Pan, C. Gu, X. Chen, W. Wang, G. Ning, L. Bian, Q. Sun, Decreased expression of SFRP2 promotes development of the pituitary corticotroph adenoma by upregulating Wnt signaling, Int. J. Oncol. 52 (2018) 1934–1946.
[29] Z. Zhang, L. Zhang, L. Zhang, L. Jia, P. Wang, Y. Gao, Association of Wnt2 and SFRP4 expression in the third trimester placenta in women with severe preeclampsia, Reprod. Sci. 20 (2013) 981–989.
[30] Y. Kawano, R. Kypta, Secreted antagonists of the Wnt signalling pathway, J. Cell Sci. 116 (2003) 2627–2634.